Acta Materialia 104 (2016) 143–155

Contents lists available at ScienceDirect

Acta Materialia

journal homepage: www.elsevier.com/locate/actamat

Full length article

Coarse-grained elastodynamics of fast moving dislocations

Liming Xiong [a, *], Ji Rigelesaiyin [a], Xiang Chen [b], Shuozhi Xu [c], David L. McDowell [c, d], Youping Chen [b]

[a] Department of Aerospace Engineering, Iowa State University, Ames, IA 50010, USA
[b] Department of Mechanical and Aerospace Engineering, University of Florida, Gainesville, FL 32608, USA
[c] Woodruff School of Mechanical Engineering, Georgia Institute of Technology, Atlanta, GA 30332, USA
[d] School of Materials Science and Engineering, Georgia Institute of Technology, Atlanta, GA 30332, USA

ARTICLE INFO

Article history:
Received 22 July 2015
Received in revised form
10 November 2015
Accepted 21 November 2015
Available online 13 December 2015

Keywords:
Atomistic simulation
Finite element
Multiscale simulations
Dislocation
Dynamic plastic deformation

ABSTRACT

The fundamental mechanism of dynamic plasticity in metallic materials subjected to shock loading remains unclear because it is difficult to obtain the precise information of individual fast moving dislocations in metals from the state-of-the-art experiments. In this work, the dynamics of sonic dislocations in anisotropic crystalline materials is explored through a concurrent atomistic-continuum modeling method. We make a first attempt to characterize the complexity of nonuniformly moving dislocations in anisotropic crystals from atomistic to microscale, including the energy intensities as well as the wavelengths of acoustic phonons emitted from sonic dislocations, and the velocity-dependent stress fluctuations around the core of nonuniformly moving dislocations. Instantaneous dislocation velocities and phonon drag effects on the dislocation motions are quantified and analyzed. Mach cones in a V-shaped pattern of the phonon wave-fronts are observed in the wake of the sonic dislocations. Analysis of simulation results based on a wavelet transform show that the faster a dislocation is moving, the longer the emitted phonon wavelength. The dislocation velocity drops dramatically with the occurrence of the interactions between dislocations and phonon waves reflected from the boundaries of specimens. The concurrent atomistic-continuum modeling framework is demonstrated to be the first multiscale method that explicitly treats the strong coupling between the long-range elastic fields away from the dislocation core, the highly nonlinear time-dependent stress field within the core, and the evolutions of the atomic-scale dislocation core structures. As such, it is shown that this method is capable in predicting elastodynamics of dislocations in the presence of inertia effects associated with sonic dislocations in micron-sized anisotropic crystalline materials from the atomic level, which is not directly accessible to the recent elastodynamic discrete dislocation model.

1. Introduction

Dynamic failure studies of materials under high strain rate loading conditions generally fall into two major categories [1,2]: dynamic fracture and dynamic plasticity. Dynamic fracture deals with the creation of new surfaces resulting from the creation of displacement discontinuities at a fraction of speed of sound in materials [2–5]. Dynamic plasticity studies relate the dynamic dislocation and/or twinning-mediated response of solids to the imposed loading at high strain rates [1,6]. Issues considered in dynamic plasticity typically include the mobility of dislocations in crystals, evolutions of dislocation density and structures, rate-controlling mechanisms of plastic flow, and so on. In particular, the plastic shearing rate for each slip system in a crystal is usually determined via the Orowan equation as the product of dislocation density, mean velocity [7], and Burgers vector. Although the dynamics of dislocations [8–14] has been the subject of intense studies for decades, the complexity of dislocations moving near and above the sonic velocity in crystals remains relatively lightly explored. The associated physical phenomena are not yet completely understood.

Extensive experiments [15–17] have successfully captured the motion of dislocations in materials under external loading, however, current experimental investigation of dynamic behavior of an individual dislocation in metallic solids is a daunting challenge due to the angstrom-scale core structure and the characteristic THz-

* Corresponding author.
E-mail address: lmxiong@iastate.edu (L. Xiong).

http://dx.doi.org/10.1016/j.actamat.2015.11.037
1359-6454/

level frequencies of the localized lattice vibrations associated with the fast moving dislocations. Direct experimental observation of sonic dislocations in solids was not possible until an alternative material, a plasma crystal, was recently developed [18–20]. Given that the inter-particle distance in plasma crystals is on the order of 100 μm or above, characteristic frequencies are on the order of 100 Hz or below, and the speed of sound in a plasma crystal is on the order of 10 mm/s [19], experiments on plasma crystals can provide qualitative understanding of dynamic behavior of sonic dislocations in certain solids [20]. However, such experiments cannot provide precise information regarding the velocity, acoustic phonon emission, or core stress fields of fast moving dislocations in crystalline metals.

In addition to experimental measurements, various theoretical models describing dislocation motion in materials have also been developed in the past 80 years. Theoretically, the physics of fast moving dislocations is complicated due to the strong coupling between the highly nonlinear short-range atomic-scale core stress fields and the long-range linear elastic stress field in the medium away from dislocation cores. Pioneering linear elastic models such as the well-known Peierls model [21], the Peierls–Nabarro model [10] or the Eshelby-Frank-Nabarro model [22] have contributed basic understanding but have ignored the nonlinearity, nonlocality, and the lattice discreteness in dislocations [7,23]. Under such simplifications, the classical Peierls model is believed to lack a drag mechanism which provides the resistance to be overcome by the applied stress to maintain dislocation motion [24]. Consequently, this model fails to predict a reasonable kinetic relation between the applied stress and dislocation velocity in materials. Such a drawback in the original Peierls model has served to motivate extensive development of increasingly sophisticated extended Peierls models [13,24–28], such as the one enhanced with a kinetic relation to include some notion of discreteness of the core structures [24]. These extended Peierls models are widely used and playing crucial roles in modeling dislocation plasticity in materials. Despite the popularity, they still account for viscous drag and the dislocation core structure in a phenomenological way, and have very limited predictive capability.

Fortunately, modern computing resources have enabled fully atomistic simulations to be employed to capture many features of dislocations, including core structures [29], migration barriers [30–34], and junction structures [35]. For fast moving dislocations, Gumbsch and Gao [36] performed the first MD simulation of stable subsonic, transonic and supersonic dislocation motion in bcc tungsten. Since then, MD simulations have been widely used to investigate the atomic-scale physical nature of sonic dislocations [37–43]. Nonetheless, existing MD simulation results are found to have significant uncertainty due to the inherent length and time scale limitations. For example, the dislocation velocity from a simulation with a smaller MD cell size was found to be slower than that from a simulation with a larger MD cell size [44]. It was also shown that a steady-state dislocation velocity in MD can be achieved only after dislocations have interacted with several reflected stress waves from the MD sample borders [45]. Although atomic-scale simulations have been very useful in elucidating the qualitative behavior and mechanisms of mobile dislocations, it is still perhaps too early to expect the establishment of the direct quantitative connections between atomistic simulations and experiments. Given the characteristic nm length scale of a dislocation core and much longer range elastic interactions with the other dislocations, the dynamic behavior of dislocations is patently multiscale. Concurrent methods that link atomistic and continuum plasticity within one model are therefore necessary to capture the interactions among the different scales in dislocation dynamics. Over the last 20 years, numerous concurrent methods have been developed to seek atomic [46–49] and even quantum level resolution [50] at a significantly lower computational cost than that offered by just MD or ab initio calculations. For example, a finite-temperature quasicontinuum approach within the framework of maximum-entropy non-equilibrium statistical mechanics has been developed [51–53]. Although the finite temperature quasicontinuum approach has been recently applied to predict dislocation velocities in materials under dynamic loadings [52], a set of phenomenological kinetic equations of the Onsager type [54–56] for heat dissipation associated with moving dislocations has been employed.

Overall, existing theoretical and computational models do not have sufficient generality to predict all three key physical aspects of moving dislocations: 1) evolution of atomic-scale core structures; 2) coupling between the highly nonlinear short-range core stress field and the long-range linear elastic stress field away from the core; 3) material inertia associated with sonic dislocations. The current study employs a concurrent atomistic-continuum (CAC) methodology [57–67] for multiresolution modeling, based on an atomistic field formalism [68–70] in which the microscopic balance equations are formulated as an extension of Irving–Kirkwood formalism [71]. In CAC, the finite element (FE) method is used to solve for the atomic displacement field in crystalline materials. The CAC method [57–67] has naturally resulted from the employment of the uniform coarse FE mesh. By embedding the local atomic structure within each material point, CAC simulations are able to reproduce dislocation nucleation and migration in materials [61–64,72]. In addition to dislocations, CAC models are also demonstrated to be capable of reproducing the full sets of phonon dispersion relations in anharmonic polyatomic crystals [66,67]. Therefore, in principle, the CAC model admits the essential dynamics of moving dislocations on length and time scales ranging from the atomic to the mesoscopic levels of microstructure and initial-boundary value problems of interest. These features distinguish the CAC method from the microcontinuum theories [73] or the other existing multiscale methods [74] and motivates application of this method to analyze sonic dislocation behavior. Comparing to our previous CAC-based studies [57–67], the novel aspects of CAC employed in this work include: 1) Quadrilateral-shaped elements are employed to discretize the 2D fcc solid, while constant strain triangular elements and hexagonal rhombohedral-shaped elements are used in the previous CAC models of fcc crystals; 2) An algorithm based on the phonon wavelet transform is developed and implemented into CAC to quantify the instantaneous wavelength, frequency and energetics of phonon waves emitted from the moving dislocations. In addition, the local kinetic temperature rise due to the fast moving dislocations is quantified in anisotropic crystalline materials.

2. Methodology and computational specimen configuration

Here we explore the complex dynamics of fast moving dislocations by considering an idealized two-dimensional (2D) lattice which resembles the atomic configuration of a fcc single crystal (Fig. 1a). Plane strain conditions are considered; atoms are not allowed to move along the $\boldsymbol{z}$-direction and are free to move in the $\boldsymbol{x}$ and $\boldsymbol{y}$ directions. The 2D models, instead of quasi-2D or 3D models, are constructed and investigated for two reasons: 1) the only existing direct experimental observation of sonic dislocation motions in solids is in 2D plasma crystals; 2) the dislocation lines in three dimensions are curved and therefore of mixed character, having both edge and screw components. The dynamics of mixed mode dislocations in an anisotropic crystal will be rather complicated because the contributions to core radiation from the edge and the screw components are strongly coupled. Thus, the 2D

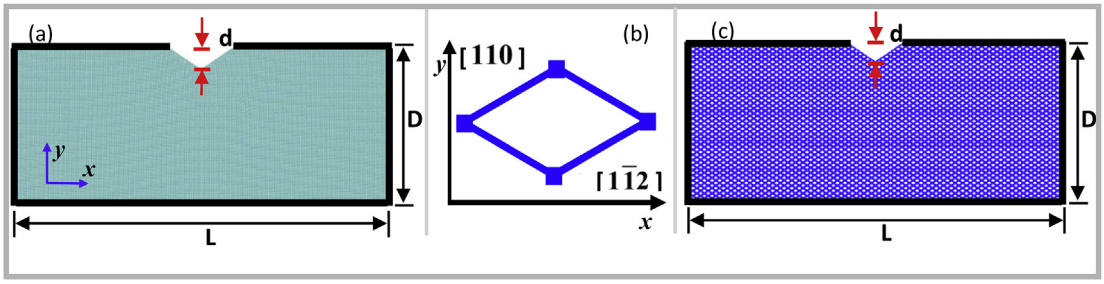

Fig. 1. Computational configuration of a notched 2D L-J solid: (a) MD; (b) 4-node FE; (c) CAC.

computational configuration eases the computational effort and aids in the visualization of dislocation motion and interaction with phonon waves at substantial length scales compared to dislocation core structure. A V-notch with a depth of ***d*** is initially introduced into the model as shown in Fig. 1a. The dimensions of the specimen are $\boldsymbol{L} = 0.54$ μm and $\boldsymbol{D} = 0.34$ μm. For both MD and CAC, three sets of models are constructed with different notch depths, **d/D** ≈ 1/10 for **Model-1**, **d/D** ≈ 1/20 for **Model-2** and **d/D** ≈ 1/40 for **Model-3**. The notch configurations with different depths, ***d***, facilitate differences in dislocation interactions with boundaries, which in turn affects the time history of nucleated dislocations. The notched single crystal is subjected to displacement-controlled tensile loading along the ***x*** (horizontal) direction by assigning rigid displacements to sets of atoms/elements on the ends. The two rigid ends along the ***x***-direction are clamped and moved at a constant velocity of 10 m/s. During the simulation, the two rigid layers stay perfectly flat while the atoms/nodes on the top and bottom edges along the ***y***-direction are net traction-free. The applied displacement is held fixed as soon as a dislocation nucleates from the notch tip; attainment of steady-state dislocation velocity is then possible since energy is still continuously being provided by the constant long-range applied stress.

When the 2D fcc solid in CAC undergoes plastic deformation via slip, only two slip directions conform to the geometry of primitive cells in 2D fcc solids. Here the finite element (FE) is a quadrilateral shape (Fig. 1b), employed to discretize the lattice. The quadrilateral-shaped element ensures that the nucleated dislocations can glide between FEs on either of two slip systems along element boundaries. In this work, each element contains 100 atoms. The atomic displacement field within each element is constrained by the FE nodal degrees-of-freedom. The resulting CAC model contains 40,000 elements (Fig. 1c) to represent 4,000,000 atoms. In order to account for the nonlinearity and nonlocality of the atomic interactions, which actually determine dislocation core structures and consequently the dislocation mobility, we use an interatomic force field as the constitutive rule in the CAC models. For simplicity, the Lennard-Jones (L-J) force field [75] is chosen. The L-J potential is used with parameters $\varepsilon = 0.167$ eV and $\sigma = 2.3151$ Å, yielding the lattice constant $a_0 = 3.616$ Å in the case Cu [75]. The L-J potential has a smooth cutoff between the fourth- and fifth-nearest neighbors at $1.49a_0$. The resulting defect configurations from L-J potential for fcc solids are found to be rather similar to those of the fully atomistic models with EAM [76–78]. Different from the traditional constitutive rules applied in linear elasticity theory or DD models, the characteristic nonlinear form of the L-J interatomic force fields not only brings atomic information into the framework of dislocation dynamics but also will naturally allow full sets of dispersive phonon frequency spectra. Thus, it admits study of the acoustic phonon emission and propagation from fast moving dislocations. The shear wave velocity in the present model with L-J interatomic interactions takes on a value of ~2700 m/s. In order to calculate the internal force density, a Gauss quadrature method [61] is used in this work although other sophisticated quadrature rules have been recently developed and implemented into CAC [79]. Here we want to emphasize that, no matter which quadrature scheme is followed, special care must be taken due to the presence of nonlinearity and nonlocality in the form of the interatomic force field.

At finite temperature, phonon waves emitted from the moving dislocations will be scattered by thermal phonons in crystalline materials. In this situation, the dynamics of fast moving dislocations in materials at non-zero temperature becomes very complicated. It is difficult to decouple and quantify the dislocation-emitted phonon waves from thermal phonons. Therefore, in this work, the initial temperature of the system is set to be 0 K but the further kinetic fluctuations of FE nodes during the simulations are not controlled; in other words, no thermostat is employed. A central difference scheme is employed for time integration. For purposes of validation, three sets of identical MD simulations for three different models are also conducted using the LAMMPS package [80]. The initial temperature of the MD system is also set to 0 K; as for CAC, there is no initial kinetic energy in these MD models. The further thermal motions of the atoms are not controlled or thermostated in the MD simulations to facilitate direct comparison. The motion of dislocations and the emission of the phonon waves are then traced by integrating the balance equation of linear momentum in CAC and the equation of motion in MD with the same time step of 5 fs. Such a small time step is sufficient to ensure numerical stability and to capture elementary high-frequency phonon emission from fast moving dislocations.

3. Simulation results

3.1. Dislocation elastodynamics

Fig. 2 compares images of time sequences of dislocation nucleation and motion from MD and CAC simulations of Model-1 (d/D = 1/10, Fig. 2a) and Model-2 (d/D = 1/20, Fig. 2b). Due to the symmetry of the specimen configuration about the ***y*** axis, only the left part of the specimen in MD and the right part of the specimen in CAC are displayed and compared. Here, the atoms in MD and the elements in CAC are color coded in displaying the normal stress component ($\boldsymbol{\sigma_{yy}}$). The color, red or blue, respectively, indicates the tensile or compressive stress along the ***y*** direction. At t = 5 ps, with the onset of the dislocation nucleation, strong stress concentrations around the notch tip are observed in both CAC and MD. Since the complex dynamics of dislocations does not come into play at this stage, the stress field from CAC is found to be almost exactly the same as that from MD. This again provides the evidence that the quasistatic CAC will accurately reproduce the static stress field around defects [79]. We also notice that maximum $\boldsymbol{\sigma_{yy}}$ in the region of high stress concentration in Model-2 is ~1.2 times that in Model-1. From t = 10 ps to t = 15 ps, the dislocations are accelerated, and

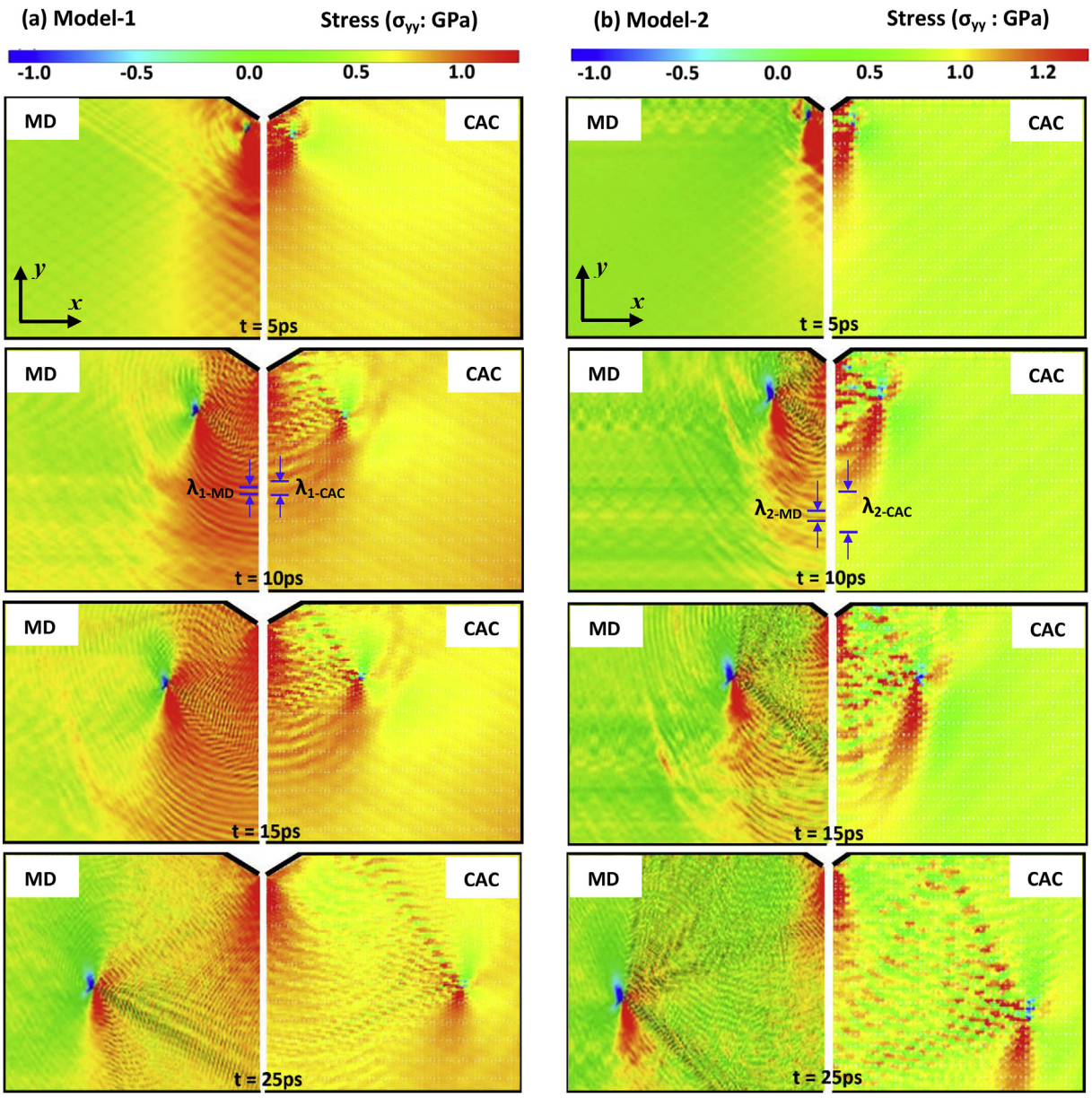

Fig. 2. Snapshots of time sequences of dislocation nucleation and motion by MD and CAC simulations in a 2D L-J solid (0.54 μm × 0.34 μm) with different notch depths: (a) Model-1 with d/D = 1/10; (b) Model-2 with d/D = 1/20.

acoustic phonon waves are emitted from the accelerating dislocations in both CAC and MD simulations. However, the wavelengths of acoustic emissions from dislocations in CAC models are always larger than those from MD simulations, that is, $\lambda_{1\text{-CAC}} > \lambda_{1\text{-MD}}$ (Fig. 2a) and $\lambda_{2\text{-CAC}} > \lambda_{2\text{-MD}}$ (Fig. 2b), because the coarse element (100 atoms/element) cuts off short wavelength phonons. When the dislocation is further accelerated to a higher velocity at t = 25 ps, the motion of the fast moving dislocations generates wave fronts that pile up around the stress discontinuity region associated with dislocations. Two types of waves, shear and compressive, emit together but are found to decouple as they radiate from the dislocations. The phonon wave radiations form a V-shaped pattern of strong lattice vibrations in the wake of the dislocations in both CAC and MD Model-1 (Fig. 2a, t = 25 ps) and Model-2 (Fig. 2b, t = 25 ps). In Fig. 2a, at t = 25 ps, such radiation is seen to form a pair of shock fronts of shear wave character, comparable to a so-called Mach cone. A Mach cone is typically formed when the object in a medium is moving faster than the speed of sound in that medium. Particularly, it is seen that the emitted waves from the fast moving dislocations eventually form a cloud and created a highly disorganized stress field in the wake of the dislocations. Contrasting with the wave patterns observed in Model-1 (Fig. 2a, t = 25 ps), two pairs of shock wave fronts are observed in Model-2 (Fig. 2b, t = 25 ps). In addition, the wings of the observed Mach cones created by the moving dislocation in Model-1 are slightly shorter than those in Model-2, and even much shorter than those in Model-3 with d/D = 1/20 as shown in Fig. 3. In addition, the Mach cone angles in the CAC and MD simulations of these three models are also found to differ slightly: the Mach cone angle in Model-3 is the smallest while that the angle in Model-1 is the largest. It is well known that longer Mach cone wings and smaller Mach cone angles signify that the object is moving faster. Hence, our CAC and MD simulation results imply that the dislocation in Model-3 with the smallest notch depth achieves the highest velocity.

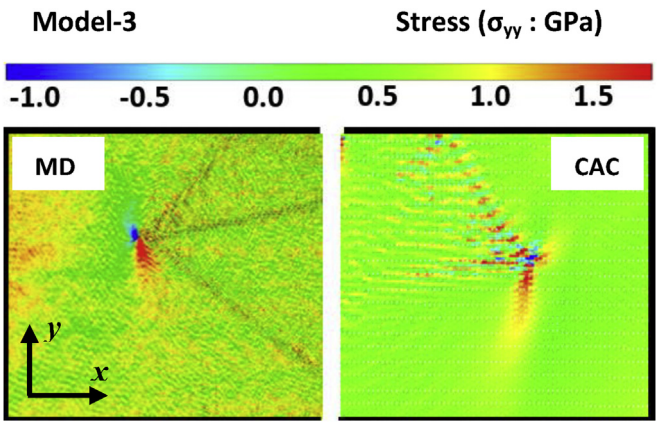

Fig. 3. Formation of Mach cones around the fast moving dislocation motions in Model-3 with d/D = 1/40 by MD and CAC simulations.

In this work, we also compute the local kinetic energies of individual atoms in MD as well as the kinetic energies of atoms embedded within each element in CAC, and then map the kinetic energies to a local kinetic temperature according to the Boltzmann relation for two degrees of freedom. Fig. 4 shows the local temperature distributions from MD and CAC simulations of dislocation motions in Model-1 and Model-2, respectively. The images are shaded according to local temperature, with the "hot" atoms (MD) or nodes (CAC) shaded red and the "cool" ones blue. A feature made visible by shading the samples according to temperature is the appearance of shock waves in the material, indicating that the dislocations travel through the material at or above sonic velocity. It is seen that the local temperature of the atoms (MD) and the nodes (CAC) participating in the dislocation glide is relatively high. High values of the local temperature at the moving dislocation core can be explained by the local transient shear processes in the slip systems. Such shear process on the slip plane gives the appreciable rise in local temperature since the shear processing time is so short that the heat may not have enough time to be dissipated throughout the specimen or radiated into the environment. Fig. 4 shows that the local temperature at the dislocation core exceeds 400 K in Model-1 and reaches more than 500 K in Model-2. However, the local temperature in the region a few atomic distances away from the dislocation is of the order of only a fraction of 1 K degree. As a consequence, the average temperature in the entire sample in Model-1 and Model-2 corresponds to ~30 and ~40 K, respectively. Visualization of the local temperature distribution in MD and CAC simulations enables us not only to quantify how much the kinetic energy of a moving dislocation is dissipated as heat, but also to recognize the patterns and energy intensities of the phonon emissions from the fast moving dislocation in anisotropic crystals subjected to high strain rate loadings. Such a heating effect of a gliding dislocation is of importance in many aspects of plastic deformation. In the past, some estimates of the maximum temperature rise due to plastic flow have been made in the literature, but it has not been calculated exactly. Here we demonstrate that CAC can incorporate explicitly the kinetic temperature field resulting from the movement of individual dislocations without the need to make assumptions on dislocation mobility laws, core structures and core stress field.

To quantify the instantaneous dislocation velocity, we first track the position of a dislocation in each set of CAC and MD simulations. The instantaneous dislocation position relative to the notch tip is recorded by computing the spatially-averaged positions of those dislocated atoms at each time step in MD as well as in CAC simulations. In CAC simulations, the atomic positions are actually mapped from the FE mesh deformation [61]. The dislocation positions are plotted as a function of time in Fig. 5 (in the web version). Fig. 5a shows the predictions from CAC simulations while Fig. 5b presents the results from MD simulations, respectively. In Model-1, the dislocation in CAC migrates ~125 nm in 50 ps while it only

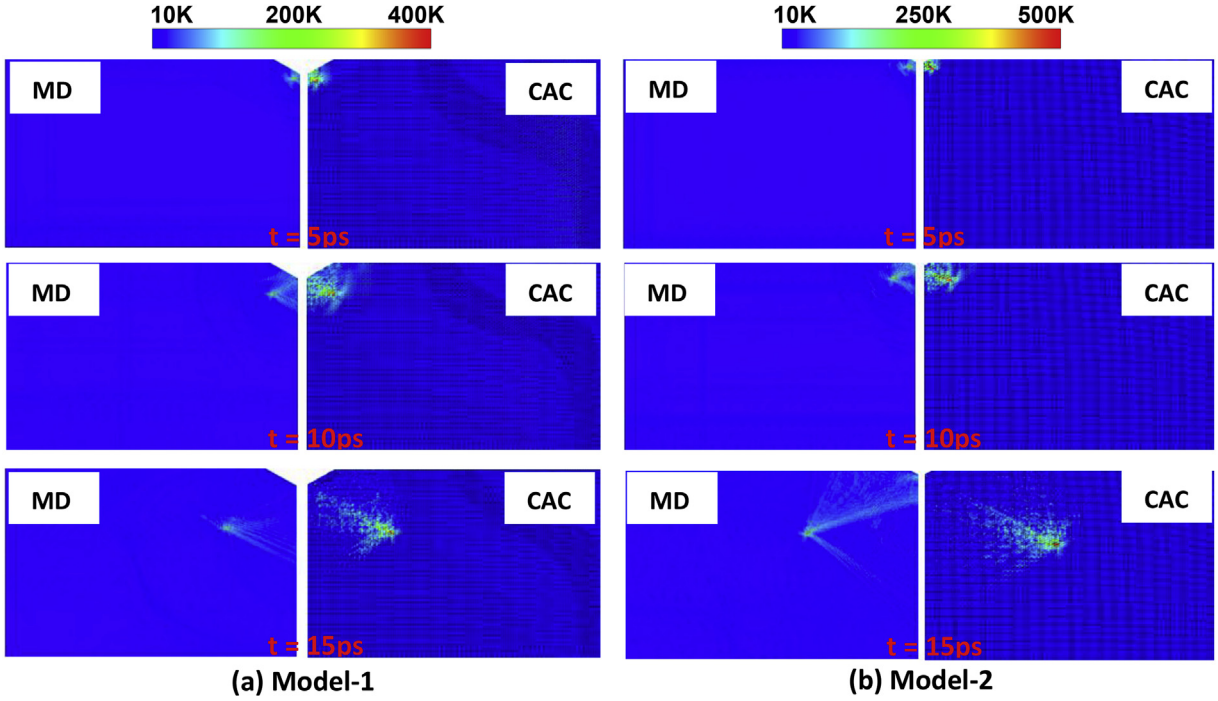

Fig. 4. Snapshots of time sequences of local temperature distributions by MD and CAC simulations in a 2D LJ solid (0.54 μm × 0.34 μm) with different notch depths: (a) Model-1 with d/D = 1/10; (b) Model-2 with d/D = 1/20.

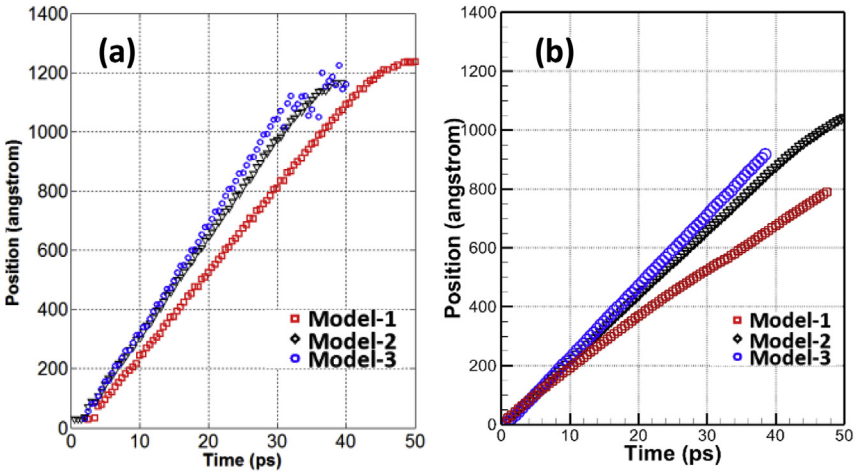

Fig. 5. Averaged dislocation positions as a function of time in three different models (Red: d/D = 1/10; Black: d/D = 1/20; and Blue: d/D = 1/40) by (a) CAC and (b) MD simulations (For interpretation of the references to colour in this figure legend, the reader is referred to the web version of this article.).

migrates 80 nm in 50 ps in MD. Similarly, in Model-2, the dislocation in CAC Model-2 migrates ~115 nm in 40 ps while it only migrates ~90 nm in 40 ps in MD. Dislocations in the CAC model move ~1.2 times faster than in full MD simulations. The overestimation of the dislocation velocity by CAC models is believed to be caused by the employment of a linear element shape function.

We then take the first derivative of the dislocation position-time curves to quantify the instantaneous velocities of dislocations. The obtained dislocation velocity-time history curves from CAC simulations of three different models are presented in Fig. 6. In the dislocation velocity-time history from all of the three models, three distinct velocity regimes can be clearly identified: 1) a transient acceleration of dislocation due to the strong stress concentration around the notch tip from t = 0 ps to t = 10 ps; 2) a plateau velocity of dislocation towards a steady-state dislocation motion from t = 10 ps to t = 35 ps in Model-1 and from t = 10 ps to t = 25 ps in Model-2, respectively; and 3) a dramatic decrease of the velocity when the dislocation approaches the sample boundaries. The transient acceleration is obviously relevant to localized stress concentrations around the notch tip. The maximum dislocation velocities in CAC Model-1, Model-2 and Model-3 are ~2900 m/s, ~3400 m/s and ~3700 m/s, respectively. These plateau velocity values range from near to well above the speed of sound (2700 m/s) in these 2D L-J solids. It is therefore concluded that nonlocality and nonlinearity in the CAC models enables description of supersonic dislocation motion which is largely inaccessible to other continuum theories. It is also confirmed that the dislocation can achieve different plateau velocities for different initial notch depths, reflecting the fact that intensity and spatial character of elastic energy release differs for each notch as the dislocation is nucleated. The sharp decrease of the dislocation velocity after the steady-state dislocation velocity is reached corresponds to the onset of interaction of reflected phonon waves from the sample boundaries with the dislocations (Fig. 2). The effective driving force for the dislocation motion is consequently decreased due to such dislocation-wave interactions. We expect that the dislocation velocity may be able to achieve an even higher value if the CAC simulation is conducted with a millimeter-sized specimen which will provide enough space for the dislocation to accelerate and run continuously within a longer observation time prior to interaction with reflected phonons.

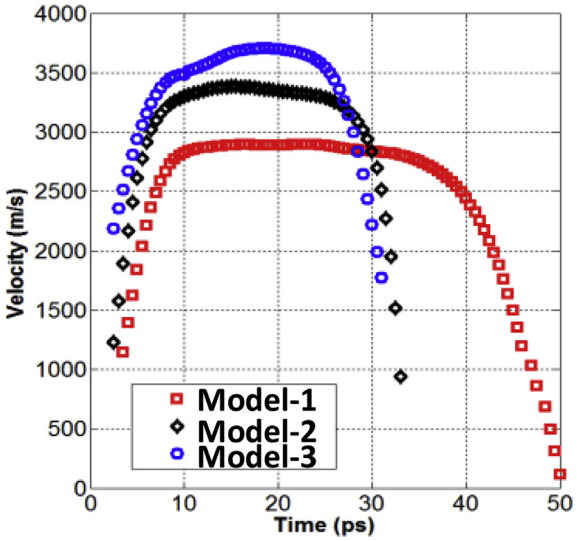

Fig. 6. Dislocation velocity-time history in three models by CAC simulations.

3.2. Acoustic phonon emission from fast moving dislocations

In addition to measuring the instantaneous dislocation velocity, another important aspect in characterizing the complex dynamics of fast moving dislocation is to quantify the instantaneous energy intensity and wavelength of the phonons emitted from moving dislocations. Although phonon radiations from dynamic crack propagation, extension of twins and fast moving dislocations have been investigated, the existing analyses are usually conducted within the framework of an isotropic elastic continuum. For an anisotropic elastic 2D fcc solids, the nonlinearity and nonlocality of the dislocation cores will introduce more complexity into the emitted transverse and longitudinal waves that propagate along different directions. Therefore, it becomes necessary to understand more about the physical nature of wavelength and frequency, propagation direction and amplitude, as well as the energy intensity of the emitted phonon waves. Here, the wavelet transform [81] is employed to analyze the dynamics and time-dependent energy intensity distribution of phonons emitted from fast moving dislocations. The wavelet transform is considered as a compromise between the spatial and Fourier domain representations of a signal. The difference is that a Fourier transform utilizes a

complex exponential basis while the wavelet basis function is employed in a wavelet transform. The wavelet transform not only provides vibrational information but also retain information on where and when those vibrations occur in a system. The first attempt of using wavelet transform to resolve the phonon motion and the energy from a vibrating ensemble of atoms in an MD simulation was recently made by Baker and co-workers [81]. It was demonstrated that the wavelet transform can provide the physical mechanisms of an ensemble of phonons within a certain spatial and wave-number range. Most importantly, the wavelet transform only involves three quantities: location, displacement, and velocities of atoms. These quantities are directly available from MD as well as the CAC simulations.

Due to the change from using continuous to discrete equations in the wavelet transform, the spatial coordinate $\boldsymbol{x}$ becomes a vector size of N ranging from $\boldsymbol{x}_1$ to $\boldsymbol{x}_N$. Here $\boldsymbol{x}_1$, $\boldsymbol{x}_2$, …, $\boldsymbol{x}_i$, …, $\boldsymbol{x}_N$ are the indices of bins constructed as shown in Fig. 7. Through this method, the analytical integration that spans all of space in a wavelet transform is approximated as a summation over these finite intervals. Then the representation of the phonon energy intensity signal is calculated and displayed in $\boldsymbol{x}$-$\boldsymbol{k}$ coordinate to visualize the localized vibrational processes (Fig. 8), where $\boldsymbol{k}$ is the wave vector. Phonon emissions from the moving dislocations in Model-2 at t = 5 ps and t = 15 ps are presented in Fig. 8a and b, respectively. Both CAC and MD simulation results show that a Gaussian envelope of phonon wave packets is emitted from the moving dislocation at a velocity of ~2900 m/s when t = 5 ps(Fig. 8a). The allowed wave vector of the emitted phonons from CAC simulations is mainly $\boldsymbol{k} = 0.2\ (2\pi/a)$ or below while that from MD simulations is seen to be mainly $\boldsymbol{k} = 0.2\ (2\pi/a)$ but can be above (Fig. 8a). This means that the present CAC simulations can only capture the emission of phonons with the wavelength being equal to or larger than $5a$ (a being the lattice constant of the lattice), while full MD models allows the emission of phonons with the wavelength being smaller than $5a$. This result thus explains why the wavelength, $\lambda_{1\text{-CAC}}$, of the stress waves from CAC simulation is larger than that, $\lambda_{1\text{-MD}}$, from MD (Fig. 2a). Although there exists a difference between CAC and MD simulation results in terms of the allowed phonon wavelength, further examination of phonon energy intensity in Fig. 8a shows that the majority of the energy is being carried by the phonons with wavelengths larger than $5a$. This gives us the confidence of using the present CAC models to approximately characterize the phonon dynamics of fast moving dislocations. As the simulation time continues, the dislocation begins to accelerate, the emitted phonon wave packet starts to propagate. Eventually some of the phonon waves scatter into the higher modes as shown in Fig. 8b. The phonon energy release from the moving dislocations obtained in CAC simulations is slightly different from that in full MD simulations. Such differences are believed to result in the higher dislocation velocity predicted by CAC than that by MD.

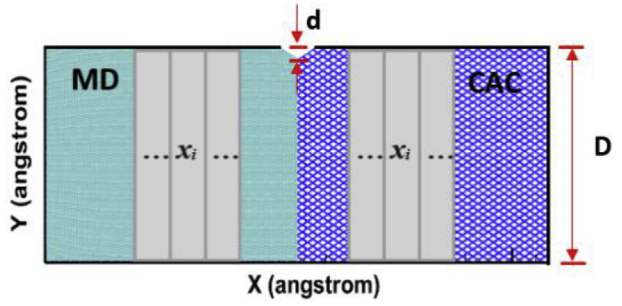

Fig. 7. Constructions of bins for wavelet transform analysis of results from MD and CAC models.

As the dislocation accelerates to ~3400 m/s at t = 15 ps, Fig. 8b presents the instantaneous phonon energy intensity distribution in the $\boldsymbol{x}$-$\boldsymbol{k}$ coordinate system. The comparison between Fig. 8b and a shows that the phonon wave packet tends to undergo a "flattening" and "shearing" process when the dislocation velocity achieves the steady-state velocity of ~3400 m/s at t = 15 ps Interestingly, both MD and CAC simulation results show that most of the phonons emitted from the dislocation at a velocity of ~3400 m/s have a wave vector of $\boldsymbol{k} = 0.2\ (2\pi/a)$ and below, which corresponds to a wavelength of $5a$ and above. The propagation of those short wavelength phonons ($\boldsymbol{k} > 0.2\ (2\pi/a)$) observed in MD at t = 5 ps (Fig. 8a) eventually become diffusive at t = 15 ps, as shown in Fig. 8b. Meanwhile, the phonon energy density distribution undergoes a transition from an orderly arrangement of mutually interfering modes (Gaussian envelope in Fig. 8a) to a less coherent structure (Fig. 8b), and is accompanied by a slight decrease in the maximum wave vector from $\boldsymbol{k}_{\max} = 0.4\ (2\pi/a)$ at t = 5 ps (Fig. 8a) to $\boldsymbol{k}_{\max} = 0.2\ (2\pi/a)$ at t = 15 ps (Fig. 8b).

The analysis based on the wavelet transform of CAC and MD results in Fig. 8 shows that the dominant wavelength of the emitted phonons from an accelerating dislocation is different from that induced by steady-state dislocation motion. It also explains why the wavelength ($\lambda_{2\text{-CAC}}$ or $\lambda_{2\text{-MD}}$) of the emitted waves from the faster dislocation ($\boldsymbol{v} \approx 3400$ m/s in Fig. 2b) is slightly larger than that ($\lambda_{1\text{-CAC}}$ or $\lambda_{1\text{-MD}}$) of the emitted waves from a slower dislocation ($\boldsymbol{v} \approx 2900$ m/s, Fig. 2a), that is, $\lambda_{2\text{-CAC}} > \lambda_{1\text{-CAC}}$ and also $\lambda_{2\text{-MD}} > \lambda_{1\text{-MD}}$. Such a dislocation velocity-dependent wavelength of the emitted phonons (the faster the dislocation, the longer the wavelength of emitted phonons) cannot be reproduced by classical continuum theories in which dispersive effects are not incorporated. In addition, the phonon wavelength analysis opens a window for us to use the present CAC models in predicting large-scale phonon dynamics associated with sonic, transonic and supersonic dislocations.

3.3. *Velocity-dependent stress field near the core of fast moving dislocations*

For dislocations moving at or near sonic velocity, the effects of core-inertia arising from phonon interactions are actually much larger than due to the viscous drag arising from the longer range field interactions outside the core because the displacement and the velocity gradient within the core are significantly larger. Therefore, the time-dependent nature of the local stress fields of fast moving dislocation cores need to be quantified before we apply coarse-grained atomistic models to simulate elastodynamic dislocation response in crystals under high strain rate deformation.

Fig. 9a and b from left to right show the results of time sequences of the shear stress field in the region of [−200 Å, 200 Å] near the core of a dislocation moving at a constant, steady-state velocity ~2900 m/s in Model-1 by CAC and MD simulations. Both CAC and MD simulation results show that the stress distribution around the fast moving dislocation cores exhibits a rich dynamic character. First of all, the stress distribution in the domain of [0, 200 Å] is obviously different from that in the domain of [−200 Å,0]. The stress in the region [−200 Å, 0] fluctuates in space while that in the [0,200 Å] domain is relatively smooth. Such 'asymmetry' is not observed in the stress distributions around static or slow moving dislocation cores. We speculate that this asymmetry in the stress distribution arises from that the emitted waves propagating forwards ([0,200 Å] domain) significantly different nature of the waves propagating backwards ([−200 Å,0] domain). The stress oscillations in [−200 Å,0] are typically induced by the phonon waves which are rippling backwards. Due to a coarse-grained

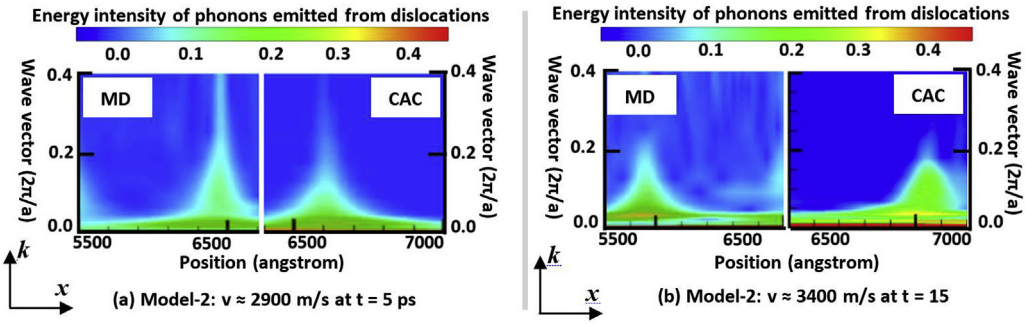

Fig. 8. Phonon energy intensity distributions associated with the acoustic waves emitted from the fast moving dislocations with velocities of: (a) $v = 2900$ m/s at t = 5 ps; and (b) $v = 3400$ m/s at t = 15 ps in Model-2 by MD and CAC simulations.

description of the atomic displacement field within the element using the linear element shape functions, the wavelength and magnitude of the stress oscillation in [−200 Å,0] from CAC simulation is slightly larger than that observed in the corresponding full MD simulation. At t = 35 ps in CAC (Fig. 9a) and t = 40 ps in MD (Fig. 9b) simulations, a 'hump' has been generated in the stress distributions in the region [0, 200 Å] because the dislocation begins to interact with the waves reflected from the boundaries of the specimen. However, the magnitude of the 'hump' from CAC simulation (t = 35 ps in Fig. 9a) again is slightly larger than that obtained from MD simulation (t = 40 ps in Fig. 9b). Such a 'hump' in the core stress field will give rise to an additional drag force on the dislocation motion and significantly decrease the dislocation velocity, as observed in Fig. 6.

To confirm that the generation of such a 'hump' in the core stress field will sharply decrease the dislocation velocity, we also plot the core stress field in Model-2 at t = 30 ps when the dislocation interacts with the reflected waves from CAC (Fig. 10a) and MD (Fig. 10b) simulations. Since the dislocation is moving at a higher supersonic velocity (~3400 m/s) in Model-2 than that (~2900 m/s) in Model-1, the wavelength of the emitted phonons in Model-2 is larger than that observed in Model-1. Hence the dislocation in Model-2 will be interacting with the reflected waves with a longer wavelength as it approaches the specimen boundaries. Consequently, the magnitude of the 'hump' generated in the core stress field (t = 30 ps for CAC in Fig. 10a and t = 25 ps for MD in Fig. 10b, Model-2) is larger than that observed in Fig. 9a–b (t = 35 ps for CAC and t = 30 ps for MD, Model-1). Obviously, the core stress field is significantly influenced by the reflections of the acoustic waves reflected from the boundaries. The successful CAC description of core stress field distortion induced by the reflected waves enables us to potentially apply the CAC model to capture the mechanical instability of dislocation cores induced by the interactions with long-wavelength waves. Such material behaviors are not directly accessible to classical MD (due to size limitations) nor to traditional DD simulations.

In Fig. 11, we demonstrate more details of the complex features of the shear stress distributions around supersonic dislocation cores. In particular, the dynamic local stress fields are reproduced from CAC and full MD simulations. Fig. 11a–c show the instantaneous stress waves (shear stress component) of steady-state dislocation motions at velocities of ~2900 m/s in Model-1 (d/D = 1/10), ~3400 m/s in Model-2 (d/D = 1/20) and ~3700 m/s in Model-3 (d/D = 1/40), respectively. Obviously, the dislocation generates more and more disturbance around the core area with increasing velocity (from Fig. 11a to c). The local shear stress field exhibits an extremely complex character due to the high dislocation velocity, as shown in Fig. 11c. Shear stress Mach cones are always seen to form behind the dislocation cores in both CAC and MD simulations. Although the wavelength of the stress waves propagating backwards in CAC simulation is found to be larger than that observed in the corresponding MD simulation, it is still encouraging to see that the complex features of the velocity-dependent core stress fields around sonic dislocations are reproduced by the present CAC method without any special treatment. Such a feature makes it possible to use the continuum CAC framework to predict plastic deformation of micron-scale specimens under shock loading where the inertial and retardation effects on the dislocation cores

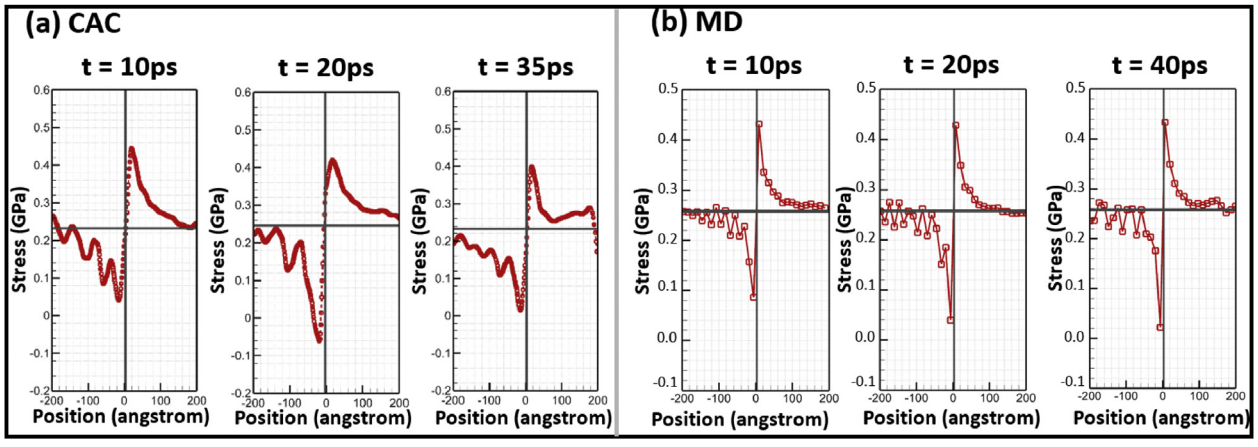

Fig. 9. Time-dependent stress component σ_{xy} near the core of a dislocation moving at a steady-state velocity of ~2900 m/s in Model-1 by (a) CAC and (b) MD simulations.

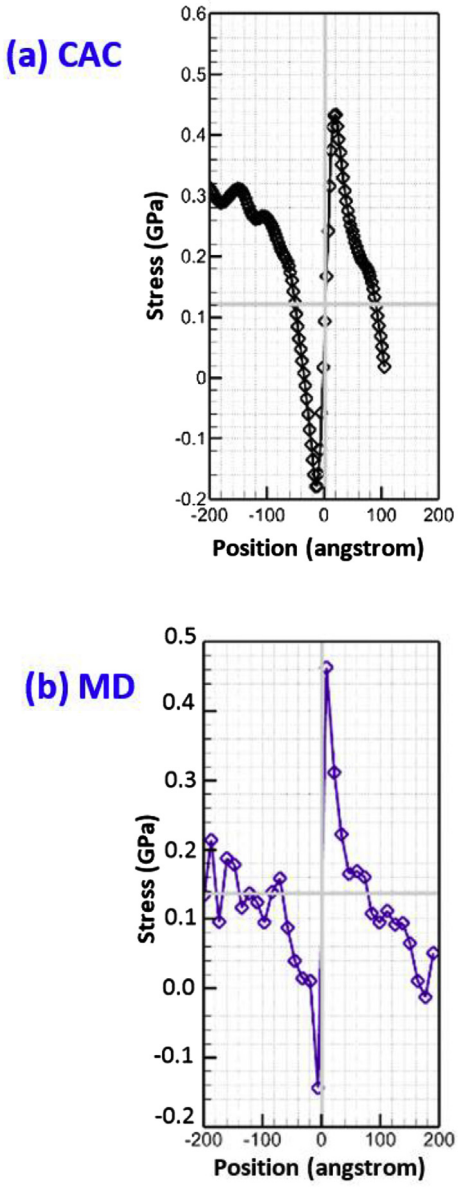

Fig. 10. Shear stress field near the cores of supersonic dislocations with a velocity of 3400 m/s in Model-2 by (a) CAC and (b) MD simulations at t = 30 ps.

are important, and the full elastodynamic field solutions (including elastic anisotropy) need to be addressed.

4. Summary and discussions

In order to predict mesoscale plasticity based on the collective behavior of a population of discrete dislocations in materials, computational Dislocation Dynamics (DD) has enjoyed the most popularity over the past few decades, constituting a major step forward in modeling mesoscale dislocation multiplication, migration and interaction [82–88]. The underlying theoretical framework of DD is the linearized theory of elasticity, used to account for long-range interactions between dislocations. Short-range dislocation interactions (e.g., junctions) are incorporated into DD by introducing empirical rules. Another common ingredient of DD is the so-called quasi-static approximation of the instantaneous stress field by considering summing the quasistatic elastic field interactions with all other dislocations in the field. Given this approximation, the term 'dynamics' in DD is a bit of misnomer since it really indicates the time evolution of dislocation structures, with kinetics limited by source multiplication, barrier bypass, and viscous drag, rather than elastodynamics [89,90]. The quasistatic approximation is believed to only be reasonable when dislocation velocities are comfortably subsonic. Such an approximation can lead to a physical dislocation behavior in materials under strong shock loading [89], since in the quasi-static approximation the dislocations are subjected to elastic interactions of dislocations ahead of the shock front. To account for drag of fast moving dislocations, a number of extended DD models have been developed in the past ten years. One of the pioneering developments is to consider the energy radiation from an accelerating dislocation through introducing an effective mass [91] or a relativistic mass [92–94] into DD methods. For shock plasticity, it may not be sufficient to correct dislocation mobility laws by such added-mass effects while still utilizing the static stress fields of dislocations for the long-range interactions. To address this issue, Balint and coworkers [89,90] have framed dynamic discrete dislocation plasticity (D3P) on the formulation of a fully time-dependent elastodynamic description of stress fields around dislocations, building upon the earlier works by Markenscoff and Clifton [11,12]. D3P considers the prior history of dislocation interactions up to a certain past instant in time based on a so-called retardation principle. For materials under shock loading, D3P eliminates spurious dislocation activity ahead of the shock front observed in traditional DD [89]. However, elastic nonlinearities and related dislocation core effects are still ignored in D3P models. The dislocation mobility laws in D3P need to be informed by atomistic simulations, and accordingly adjusted for dislocation migration at high velocities. The Field Dislocation Mechanics (FDM) [95–99] is a recently developed continuous field method for modeling dislocation evolution at the mesoscale which serves as an alternative to DD, although limited in capturing long range interactions of dislocations by comparison to DD. FDM can employ the full dynamic Green's function for the time-dependent core stress field of dislocations. In FDM, the small time delay of stress wave propagations associated with fast moving dislocations can be captured and the spurious dislocation nucleation ahead of the shock front (i.e., causality violation) can be avoided. However, the implementation of a fully dynamic Green's function significantly slows down the solver with the increasing number of dislocation segments during the simulations. Moreover, FDM also needs the mobility laws and short-range interaction rules as the input to describe the evolution of dislocation structures over time.

In comparisons with DD models, without the need of mobility laws or dislocation interaction rules, the CAC model presented in this work quantifies the elastodynamic complexity of dislocations at a sonic velocity in crystals from the atomic level. The CAC method is a FE implementation of the atomistic field formalism in which atomic motions are governed by the field descriptions of the linear momentum balance. Most importantly, CAC models can predict the dynamic behavior of sonic dislocations and admit full coupling between the time-dependent long-range linear elastic field away from the cores and the instantaneous highly nonlinear short-range stress field within the core. To examine the applicability of the CAC method in producing the correct dynamics of fast moving dislocation, we have quantified the time-dependent dislocation velocity, wavelength and energy intensity of emitted phonons, and the time-dependent core stress field of the moving dislocation from CAC simulations. The results are directly compared with those from the identical full MD simulations. It is shown that CAC models can be used to predict dislocation velocity and also quantify the acoustic phonon emission from moving dislocations, albeit with higher steady-state velocities owing to the coarse-grained formulation

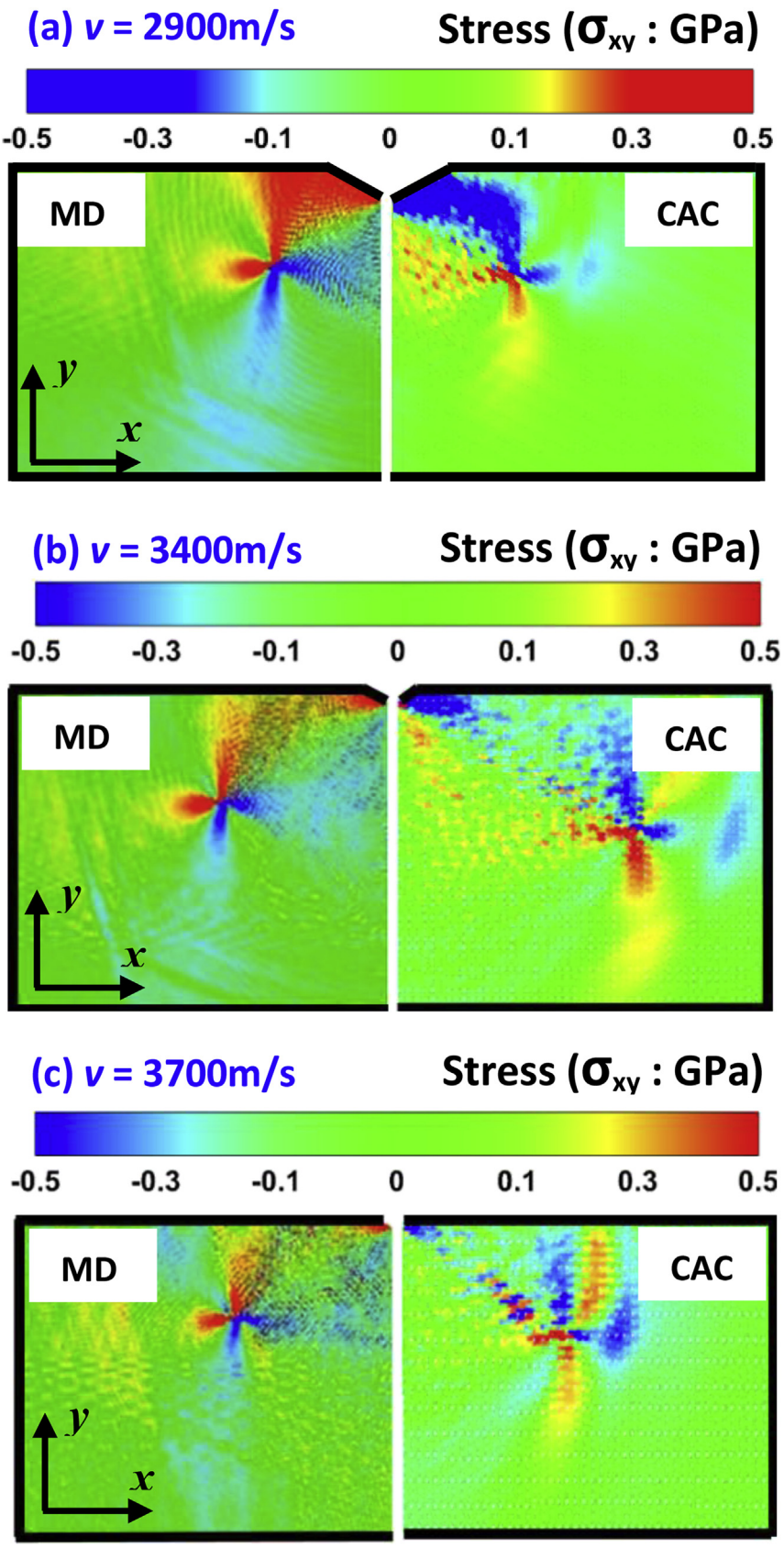

Fig. 11. Shear stress field around the cores of supersonic dislocations by CAC and MD simulations: (a) $v = 2900$ m/s; (b) $v = 3400$ m/s; and (c) $v = 3700$ m/s.

Table 1
Comparisons of MD and CAC simulations of dislocation dynamics in Model-1 and Model-2.

	Dislocation velocity MD/CAC	Phonon wavelength MD/CAC	Local temperature rise MD/CAC
Model-1	2400/2900 (m/s)	3a/5a	~350 K/400 K
Model-2	2800/3400 (m/s)	5a/8a	~400 K/500 K

and cutoff of higher frequency spectrum of phonons; this cutoff is the price to be paid for coarse-graining. The formation of Mach cones is observed for sonic dislocations. Although it seems that CAC does not retain the complete thermal vibrations from the dynamics of fast moving dislocations, it was demonstrated that CAC can capture the local kinetic temperature rise induced by the dislocation motions. The reason is that the dominant wavelengths of the emitted phonon waves from a steady-state dislocation in two-dimensional 2D L-J solid are equal to or larger than 5*a* (*a* being the lattice constant). Most importantly, we found that the faster the dislocation is moving, the longer the wavelength of the emitted phonons will be. Such a dislocation velocity-dependent wavelength of the emitted phonons necessitates the further development of the CAC model which can easily scale up in length to assure the occurrence of the stable supersonic dislocation motion in an observable time window. In addition, without the need of any additional rules beyond the interatomic force field, the CAC models are shown to be able to capture the stress wave radiation backwards from a moving dislocation core. Such radiation leads to an asymmetric localized time-dependent core stress field that strongly affects the effective drag on the dislocation.

All of these complex features of the dynamics of fast moving dislocations derived from application of the CAC method are obtained through the FE implementation of an atomistic field formalism without sophisticated constitutive modifications such as velocity-weakening or rate-and-state dependent friction. There is therefore practical difficulty within the framework of CAC [61–71] in tackling complex dislocation dynamics. Such simulations can expand upon the classical explanation by the well-established theoretical models [8–12], and to compare with and perhaps inform recently developed continuum approaches including D3P developed by Balint and co-workers [89,90] for elastodynamic dislocations.

In comparisons with MD, although the number of degrees of freedom in CAC has been significantly reduced to 1% of that of full MD simulations, both CAC and MD simulations show more disturbance around the core area as the dislocation velocity increases in the sonic range. Most importantly, the CAC results for dislocation velocities, phonon wavelength and local temperature rise summarized in Table 1 are qualitatively comparable with those from the fully atomistic simulations. In order to demonstrate the applicability of CAC to model the dislocation dynamics in more realistic metallic materials, we also implemented an EAM interatomic force field [77,78] into CAC. With the electron densities of the atoms embedded within elements being interpolated from the electron densities of the atoms embedded within the FE nodes, the efficiency of the CAC model with EAM remains the same as that of the CAC model with L-J. Fig. 12 shows that the pattern of the phonon waves emitting from the moving dislocations in 2D EAM solids are qualitatively the same with that in 2D L-J fcc solids (Fig. 3a). In

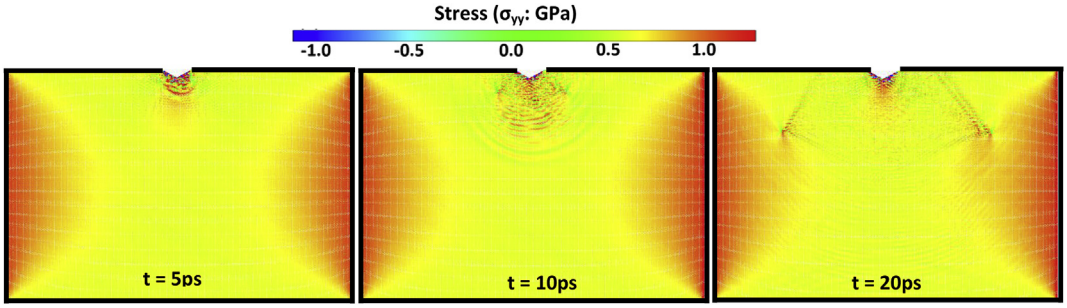

Fig. 12. Snapshots of time sequences of dislocation nucleation and motion by CAC simulations of a 2D EAM L-J solid (0.54 μm × 0.34 μm): Model-1 with d/D = 1/10.

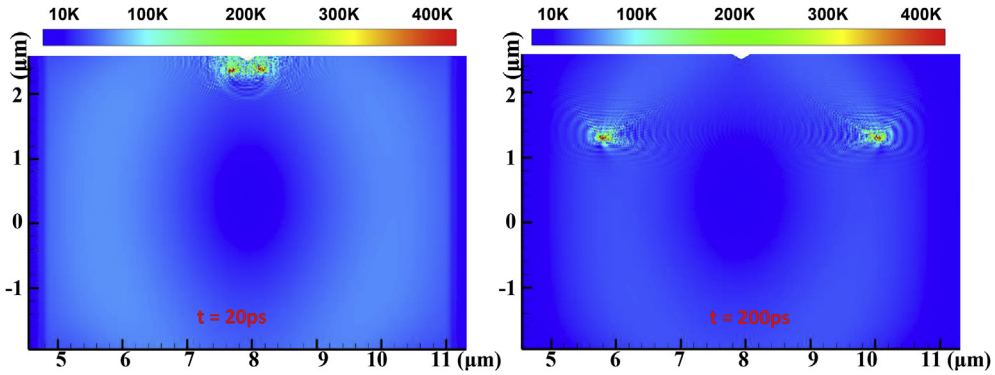

Fig. 13. Snapshots of time sequences of local temperature distributions by CAC simulations of a micron-sized 2D L-J solid (6.5 μm × 4.5 μm) with different notch depths: 153,527 elements for 0.552 billion atoms.

addition, in order to demonstrate the efficacy of coarse-graining in CAC to explore the dislocation dynamics in larger systems which are beyond the reach of fully atomistic simulations, one set of CAC simulation (153,527 elements) of dislocation motions in a micron-sized 2D LJ solid (6.5 μm × 4.5 μm, 552,697,200 atoms) is also performed in this work. The local temperature rise induced by the sonic dislocation motions in such as micron-sized anisotropic crystal is presented in Fig. 13. Since the EAM potential not only describes well the elastic constants and basic energetics but also the phonon frequency spectra in metallic materials, it provides a more accurate propagation of the phonon waves. Figs. 12 and 13 show that there will be no conceptual challenges to extend the present CAC models to simulate the complexity of moving dislocations in more realistic materials at the microscopic level.

The results presented in this work will provide us a basis for future detailed studies of the role of our multiscale simulations of defect dynamics in materials from atomic to microscopic level. However, one source of overhead of the CAC method is its cost of algorithm development and numerical implementations, like most "home-grown" multiscale modeling methods which "mainly exist as research-level codes within individual research teams" [100]. From the theory and methodology development standpoint [101], one of the ultimate objectives of the further development of CAC or other sophisticated multiscale simulation tools such as CADD [47] is to predict the dynamic properties of dislocations from the underlying atomistic processes, preferably with no adjustable parameters, not only in a simple sample material as presented in this work but also the realistic materials with complex microstructures. Although various multiscale methods have been developed in the past decades, it should be noted that the feasibility of the deployment of these multiscale methods in computational material design still depends on a successful resolution of several challenges. The foremost challenge is our ability to significantly improve the accuracy and efficiency of the multiscale models. A second challenge is to bridge the gap between multiscale models and experiments. There still exists a significant difference between the time and length scales accessible to present multiscale simulations which can reach down to atomic scales and those pertinent to the state art of microscopic experiments including *in situ* and atomic-scale resolution techniques. The third and the final challenge is to incorporate the microstructure effects into multiscale models to understand the activities of defects in heterogeneous materials. The development of more efficient concurrent atomistic-continuum methods for larger length-scale (e.g., >1 μm) modeling of materials with complex microstructures is therefore of high priority, as well as consideration of longer time scales.

Acknowledgments

This material is based upon the work supported by US National Science Foundation as a collaborative effort under Award Numbers CMMI-1232878 (SX, DLM) & CMMI-1233113 (YC), and the work supported by the U.S. Department of Energy, Office of Basic Energy Sciences, Division of Materials Sciences and Engineering under Award Number DE-SC0006539(XC and LX). The CAC computer code in its present form is a culmination of developments supported in part by National Science Foundation under Award Number CMMI-1129976 and by Defense Advanced Research Projects Agency under Award Number N66001-10-1-4018. JR also acknowledges the support from National Science Foundation under Award Number CMMI-1536925 and the CyEnce-ISU supercomputing resources provided by Prof. Arun Somani from the Department of Electrical and Computer Engineering at Iowa State University. This work also used the Extreme Science and Engineering Discovery Environment (XSEDE), which is supported by National Science Foundation grant number ACI-1053575.

References

[1] R.J. Clifton, Dynamic plasticity, ASME J. Appl. Mech. 50 (1983) 941–952.
[2] A.J. Rosakis, G. Ravichandran, Dynamic failure mechanics, Int. J. Solids Struct. (2000) 331–348.
[3] G. Ravichandran, R.J. Clifton, Dynamic fracture under plane wave loading, Int. J. Fract. 40 (1989) 157–201.
[4] L. Lambros, A.J. Rosakis, Shear dominated transonic interfacial crack growth in a biomaterial-I. Experimental observations, J. Mech. Phys. Solids 43 (1995) 169–188.
[5] H. Gao, Y. Huang, P. Gumbsch, A.J. Rosakis, On radiation-free transonic motion of cracks and dislocations, J. Mech. Phys. Solids 47 (1999) 1941–1961.
[6] K.T. Ramesh, Effects of high rates of loading on the deformation behavior and failure mechanisms of hexagonal close-packed metals and alloys, Metall. Mater. Trans. A 33 (3) (2002) 927–935.
[7] J.P. Hirth, J. Lothe, Theory of Dislocations, Wiley, New York, 1982.
[8] F.C. Frank, Sessile dislocations, Proc. Phys. Soc. 62 (1949) 202–203. London, Sect. A.
[9] J.D. Eshelby, Uniformly moving dislocations, Proc. Phys. Soc. 62 (1949) 307–314. London, Sect. A.
[10] F.R.N. Nabarro, Dislocation in a simple cubic lattice, Proc. Phys. Soc. 59 (1947) 256–272.
[11] X. Markenscoff, The transient motion of a nonuniformly moving dislocation, J. Elast. 10 (1980) 193–201.
[12] X. Markenscoff, R.J. Clifton, The nonuniformly moving edge dislocation, J. Mech. Phys. Solids 29 (1981) 253–262.
[13] Y.P. Pellegrini, Dynamic Peierls–Nabarro equations for elastically isotropic crystals, Phys. Rev. B 81 (2010) 024101.
[14] Y.P. Pellegrini, Equation of motion and subsonic-transonic transitions of rectilinear edge dislocations: a collective-variable approach, Phys. Rev. B 90 (2014) 054120.
[15] K.M. Jassby, T. Vreeland, Dislocation mobility in copper and zinc at 44K, Scripta Metall. 5 (1971) 1007.
[16] P. Kumar, R.J. Clifton, Dislocation motion and generation in LiF single crystals subjected to plate impact, J. Appl. Physics 50 (7) (1979) 4747–4762.
[17] S.K. Kim, R.J. Clifton, Dislocation motion in MgO crystals under plate impact, J. Mater. Science 19 (5) (1984) 1428–1438.
[18] C.H. Chiang, I. Lin, Cooperative particle motions and dynamical behaviors of free dislocations in strongly coupled quasi-2D dusty plasmas, Phys. Rev. Lett. 77 (1996) 647.
[19] V. Nosenko, S. Zhdanov, G. Morfill, Supersonic dislocations observed in a plasma crystal, Phys. Rev. Lett. 99 (2007) 025002.
[20] V. Nosenko, G.E. Morfill, P. Rosakis, Direct experimental measurement of the speed-stress relation for dislocations in a plasma crystal, Phys. Rev. Lett. 106 (2011) 155002.
[21] E.R. Peierls, The size of a dislocation, Proc. Phys. Soc. Lond. 52 (1940) 34.
[22] J.D. Eshelby, F.C. Frank, F.R.N. Nabarro, The equilibrium of linear arrays of dislocations, Philos. Mag. 42 (327) (1951) 351–364.
[23] J. Weertman, J.R. Weertman, Moving dislocations, in: F.R.N. Nabarro (Ed.), Dislocations in Solids, 3, 1980 ch. 8, pp. 3–59. The Netherlands: North-Holland, Amsterdam.
[24] P. Rosakis, Supersonic dislocation kinetics from an augmented Peierls model, Phys. Rev. Lett. 86 (2001) 95–98.
[25] J. Lothe, J.P. Hirth, Dislocation dynamics at low temperatures, Phys. Rev. 115 (3) (1959) 543.
[26] R. Miller, R. Phillips, G. Beltz, M. Ortiz, A non-local formulation of the Peierls dislocation model, J. Mech. Phys. Solids 46 (10) (1998) 1845–1867.
[27] G. Schoeck, Peierls energy of dislocations: a critical assessment, Phys. Rev. Lett. 82 (11) (1999) 2310.
[28] R.C. Picu, The Peierls stress in non-local elasticity, J. Mech. Phys. Solids 50 (4) (2002) 717–735.
[29] H.B. Huntington, J.E. Dickey, R. Thomson, Dislocation energies in NaCl, Phys. Rev. 100 (1955) 1117.
[30] V.B. Shenoy, R. Phillips, Finite-sized atomistic simulations of screw dislocations, Philos. Mag. A 76 (1997) 367–385.
[31] S. Rao, C. Hernandez, J.P. Simmons, T.A. Parthasarathy, C. Woodward, Green's function boundary conditions in two-dimensional and three-dimensional atomistic simulations of dislocations, Philos. Mag. A 77 (1998) 231–256.
[32] V.V. Bulatov, O. Richmond, M.V. Glazov, An atomistic dislocation mechanism of pressure-dependent plastic flow in aluminum, Acta Mater. 47 (1999) 3507–3514.
[33] D.L. Olmsted, K.Y. Hardikar, R. Phillips, Lattice resistance and Peierls stress in finite size atomistic dislocation simulations, Model. Simul. Mater. Sci. Eng. 9 (2001) 215.
[34] K.W. Jacobson, J. Schiotz, Computational materials science: nanoscale plasticity, Nat. Mater. 1 (2002) 15–16.
[35] D. Rodney, R. Phillips, Structure and strength of dislocation junctions: an atomic level analysis, Phys. Rev. Lett. 82 (1999) 1704.
[36] P. Gumbsch, H. Gao, Dislocations faster than the speed of sound, Science 283 (1999) 965.
[37] H. Koizumi, H.O.K. Kirchner, T. Suzuki, Lattice wave emission from a moving dislocation, Phys. Rev. B 65 (2002) 214104.

[38] E. Bringa, A. Caro, Y. Wang, M. Victoria, J. McNaney, B. Remington, R. Smith, B. Torralva, H. Van Swygenhoven, Ultrahigh strength in nanocrystalline materials under shock loading, Science 309 (2005) 1838.
[39] E. Bringa, K. Rosolankova, R. Rudd, B. Remington, J. Wark, M. Duchaineau, D. Kalantar, J. Hawreliak, J. Belak, Shock deformation of face-centered-cubic metals on subnanosecond timescales, Nat. Mater. 5 (2006) 805–809.
[40] E. Bitzek, P. Gumbsch, Dynamic aspects of dislocation motion: atomistic simulations, Mater. Science Eng. A 400–401 (2005) 40–44.
[41] Z. Jin, H. Gao, P. Gumbsch, Energy radiation and limiting speeds of fast moving edge dislocations in tungsten, Phys. Rev. B 77 (2008) 094303.
[42] H. Tsuzuki, P.S. Branicio, J.P. Rino, Molecular dynamics simulation of fast dislocations in copper, Acta Mater. 57 (2009) 1843–1855.
[43] H.J. Chu, J. Wang, I.J. Beyerlein, Anomalous reactions of a supersonic coplanar dislocation dipole: Bypass or twinning? Scripta Mater. 67 (2012) 69–72.
[44] D.L. Olmsted, L.G. Hector, W.A. Curtin, R.J. Clifton, Atomistic simulations of dislocation mobility in Al, Ni and Al/Mg alloys, Model. Simul. Mater. Sci. Eng. 13 (2005) 371–388.
[45] C.R. Weinberger, Dislocation drag at the nanoscale, Acta Mater. 58 (2010) 6535–6541.
[46] E.B. Tadmor, M. Ortiz, R. Phillips, Quasicontinuum analysis of defects in solids, Philos. Mag. A 73 (6) (1996) 1529–1563.
[47] L.E. Shilkrot, W.A. Curtin, R.E. Miller, A coupled atomistic/continuum model of defects in solids, J. Mech. Phys. Solids 50 (2002) 2085–2106.
[48] X. Li, W.E, Multiscale modeling of the dynamics of solids at finite temperature, J. Mech. Physics Solids 53 (7) (2005) 1650–1685.
[49] R. Gracie, T. Belytschko, Concurrently coupled atomistic and XFEM models for dislocations and cracks, Int. J. Numer. Methods Eng. 78 (3) (2008) 354–378.
[50] F.F. Abraham, J.Q. Broughton, N. Bernstein, E. Kaxiras, Spanning the continuum to quantum length scales in a dynamic simulation of brittle fracture, Europhys. Lett. 44 (1998) 783.
[51] Y. Kulkarni, J. Knap, M. Ortiz, A variational approach to coarse graining of equilibrium and non-equilibrium atomistic description at finite temperature, J. Mech. Phy. Solid 56 (2008) 1417–1449.
[52] G. Venturini, K. Wang, I. Romero, M.P. Ariza, M. Ortiz, Atomistic long-term simulation of heat and mass transport, J. Mech. Phys. Solids 73 (2014) 242–268.
[53] M. Ponga, M. Ortiz, M.P. Ariza, Finite-temperature nano-equilibrium quasicontinuum analysis of nanovoid growth in copper at low and high strain rates, Mech. Mater. 90 (2015) 253–267.
[54] L. Onsager, Reciprocal relations in irreversible processes. I, Phys. Rev. 37 (4) (1931) 405–426.
[55] L. Onsager, Reciprocal relations in irreversible processes. II, Phys. Rev. 38 (12) (1931) 2265–2279.
[56] S.R. De Groot, P. Mazur, Non-equilibrium Thermodynamics, 1962. North-Holland, Amsterdam.
[57] L. Xiong, Y. Chen, J.D. Lee, Simulation of dislocation nucleation and motion in single crystal magnesium oxide by a field theory, Comput. Mater. Sci. 42 (2008) 168–177.
[58] L. Xiong, Y. Chen, Coarse-grained simulations of single-crystal silicon, Model. Simul. Mater. Sci. Eng. 17 (035002) (2009) 1–17.
[59] L. Xiong, Y. Chen, Multiscale modeling and simulation of single-crystal MgO through an atomistic field theory, Int. J. Solids Struct. 46 (2009) 1448–1455.
[60] L. Xiong, Y. Chen, J.D. Lee, A continuum theory for modeling the dynamics of crystalline materials, J. Nanosci. Nanotech 9 (2009) 1242–1245.
[61] L. Xiong, G. Tucker, D.L. McDowell, Y. Chen, Coarse grained atomistic simulations of dislocations, J. Mech. Phys. Solids 59 (2011) 160–177.
[62] L. Xiong, D.L. McDowell, Y. Chen, Nucleation and growth of dislocation loops in Cu, Al and Si by a concurrent atomistic-continuum method, Scripta Mater. 67 (2012) 633–636.
[63] L. Xiong, Q. Deng, G. Tucker, D.L. McDowell, Y. Chen, Coarse-grained atomistic simulations in Al, Ni and Cu crystals, Int. J. Plast. 38 (2012) 86–101.
[64] L. Xiong, Q. Deng, G. Tucker, D.L. McDowell, Y. Chen, A concurrent scheme for passing dislocations from atomistic to continuum domains, Acta Mater. 60 (2012) 899–913.
[65] L. Xiong, Y. Chen, Coarse grained atomistic modeling and simulation of inelastic material behavior, Acta Mech. Solida Sin. 25 (3) (2012) 244–261.
[66] L. Xiong, Y. Chen, Predicting phonon properties of 1D polyatomic chains through the concurrent atomistic-continuum simulations, Arch. Appl. Mech. 84 (9–11) (2014) 1665–1675.
[67] L. Xiong, D.L. McDowell, Y. Chen, Phonon drag on dislocations by coarse-grained atomistic simulations, Int. J. Plast. 55 (2014) 268–278.
[68] Y. Chen, Local stress and heat flux in atomistic systems involving three-body forces, J. Chem. Physics 124 (2006) 054113.
[69] Y. Chen, Reformulation of microscopic balance equations for multiscale materials modeling, J. Chem. Physics 130 (2009) 134706.
[70] Y. Chen, J.D. Lee, Y. Lei, L. Xiong, A multiscale field theory: Nano/micro materials, in: G.C. Shih (Ed.), Molecular and Continuum Mechanics: Interaction of Time and Size from Macro to Nano, Springer, 2007, pp. 23–65.
[71] J. Irving, J. Kirkwood, The statistical mechanical theory of transport processes. IV., the equations of hydrodynamics, J. Chem. Phys. 8 (1950) 817–829.
[72] Q. Deng, L. Xiong, Y. Chen, Coarse-graining atomistic dynamics of brittle fracture by finite element method, Int. J. Plast. 26 (9) (2010) 1402–1414.
[73] Y. Chen, J.D. Lee, A. Eskandarian, Atomistic counterpart of micromorphic theory, Acta Mech. 161 (1–2) (2003) 81–102.
[74] Y. Chen, J. Zimmerman, A. Krivtsov, D.L. McDowell, Assessment of atomistic coarse-graining methods, Int. J. Eng. Science 49 (2011) 1337–1349.
[75] M.D. Kluge, D. Wolf, J.F. Lutsko, S.R. Phillpot, Formalism for the calculation of local elastic constants at grain boundaries by means of atomistic simulation, J. Appl. Phys. 67 (1990) 2370.
[76] H. Kimizuka, H. Kaburaki, F. Shimizu, J. Li, Crack-tip dislocation nanostructures in dynamical fracture of fcc metals: a molecular dynamics study, J. Computer-Aided Mater. Des. 10 (2003) 143–154.
[77] M.S. Daw, M.I. Baskes, Embedded-atom method: derivation and application to impurities, surfaces, and other defects in metals, Phy. Rev. B 29 (1984) 6443.
[78] Y. Mishin, M.J. Mehl, D.A. Papaconstantopoulos, A.F. Voter, J.D. Kress, Structural stability and lattice defects in copper: ab initio, tight-binding and embedded-atom calculation, Phys. Rev. B 63 (2001) 224106.
[79] S. Xu, R. Che, L. Xiong, Y. Chen, D.L. McDowell, A quasistatic implementation of the concurrent atomistic-continuum method for fcc crystals, Int. J. Plast. 72 (2015) 91–126.
[80] S. Plimpton, Fast parallel algorithms for short-range molecular dynamics, J. Comput. Phys. 117 (1) (1995).
[81] C.H. Baker, D.A. Jordan, P.M. Norris, Application of the wavelet transform to nanoscale thermal transport, Phys. Rev. B 86 (2012) 104306.
[82] R.J. Amodeo, N.M. Ghoniem, Dislocation dynamics. I. A proposed methodology for deformation micromechanics, Phys. Rev. B 41 (1990) 6958–6967.
[83] R.J. Amodeo, N.M. Ghoniem, Dislocation dynamics. II. Applications to the formation of persistent slip bands, planar arrays, and dislocation cells, Phys. Rev. B 41 (1990) 6968–6976.
[84] E. Van der Giessen, A. Needleman, Discrete dislocation plasticity: a simple planar model, Model. Simul. Mater. Sci. Eng. 3 (1995) 689–735.
[85] V. Bulatov, F. Abraham, L. Kubin, B. Devincre, S. Yip, Connecting atomistic and mesoscale simulations of crystal plasticity, Nature 391 (1998) 669–672.
[86] H.M. Zbib, F. Rhee, J.P. Hirth, On plastic deformation and the dynamics of 3D dislocations, Int. J. Mech. Sci. 40 (1998) 113–127.
[87] W. Cai, V.V. Bulatov, J. Chang, J. Li, S. Yip, Dislocation core effects on mobility, in: F.R.N. Nabarro (Ed.), Dislocations in Solids, 2004. North-Holland, Amsterdam.
[88] S. Groh, E.B. Marin, M.F. Horstmeyer, H.M. Zbib, Multiscale modeling of the plasticity in an aluminum single crystal, Int. J. Plast. 25 (8) (2009) 1456–1473.
[89] B. Gurrutxaga-Lerma, D.S. Balint, D. Dini, D.E. Eakins, A.P. Sutton, A dynamic discrete dislocation plasticity method for the simulation of plastic relaxation under shock loading, Proc. R. Soc. A 469 (2013).
[90] B. Gurrutxaga-Lerma, D.S. Balint, D. Dini, D.E. Eakins, A.P. Sutton, Attenuation of the dynamic yield point of shocked aluminum using elastodynamic simulations of dislocation dynamics, Phys. Rev. Lett. 114 (2015) 174301.
[91] J.P. Hirth, H.M. Zbib, J. Lothe, Forces on high velocity dislocations, Model. Simul. Mater. Sci. Eng. 6 (1998) 165–169.
[92] H.M. Zbib, T. Diaz de la Rubia, A multiscale model of plasticity, Int. J. Plast. 18 (2002) 1133–1163.
[93] M.A. Shehadeh, E.M. Bringa, H.M. Zbib, J.M. McNaney, B.A. Remington, Simulation of shock induced plasticity including homogeneous and heterogenous dislocation nucleations, Appl. Phys. Lett. 89 (2006) 171918.
[94] M.A. Shehadeh, Multiscale dislocation dynamics simulations of shock-induced plasticity in small volumes, Philos. Mag. 92 (2012) 1173–1197.
[95] A. Acharya, A model of crystal plasticity based on the theory of continuously distributed dislocations, J. Mech. Phys. Solids 49 (4) (2001) 761–784.
[96] A. Acharya, Driving forces and boundary conditions in continuum dislocation mechanics, Proc. R. Soc. Lond. Ser. A 459 (2034) (2003) 1343–1363.
[97] A. Acharya, Constitutive analysis of finite deformation field dislocation mechanics, J. Mech. Phys. Solids 52 (2) (2004) 301–316.
[98] A. Acharya, New inroads in an old subject: plasticity, from around the atomic to the macroscopic scale, J. Mech. Phys. Solids 58 (5) (2010) 766–778.
[99] A. Acharya, Micro canonical entropy and mesoscale dislocation mechanics and plasticity, J. Elast. 104 (1–2) (2011) 23–44.
[100] F. Pavia, W.A. Curtin, Parallel algorithm for multiscale atomistic/continuum simulations using LAMMPS, Model. Simul. Mater. Sci. Eng. 23 (2015), 055002 (23pp).
[101] D.L. McDowell, Viscoplasticity of heterogeneous metallic materials, Mater. Sci. Eng. R. Rep. 62 (2008) 67–123.